Molecular & Cellular Toxicology
https://doi.org/10.1007/s13273-023-00418-2

ORIGINAL ARTICLE

LINC00174 targeting miR-486-5p/EIF5A2 is an oncogenic driver in oral squamous cell carcinoma

Xiao Feng[1] · Jia Tu[1] · Yan Guan[1]

Accepted: 21 November 2023

Abstract

Background Long non-coding RNAs (lncRNAs) participate in the initiation and progression of oral squamous cell carcinoma (OSCC). Although lncRNA LINC00174 plays key roles in multiple cancers, its function in OSCC has not yet been reported. This study aimed to clarify LINC00174 function and mechanism of action in OSCC.

Methods Expression analyses of LINC00174, miR-486-5p, and EIF5A2 mRNA were performed using RT-qPCR. EIF5A2 protein levels were quantified using western blot. Cell growth was investigated by performing CCK-8 and colony formation assays. Cell migration was investigated using wound healing assays. In vivo tumor formation and growth were determined by establishing animal models. The putative binding association between miR-486-5p and LINC00174 or EIF5A2 was verified using dual-luciferase or RIP assays.

Results LINC00174 and EIF5A2 were overexpressed, while miR-486-5p was poorly expressed in OSCC. Knockdown of LINC00174 expression in OSCC cells impaired proliferation, colony formation, and migration. In animal models, too, LINC00174 absence decelerated tumor development. Further mechanistic investigation showed that LINC00174 acted as a functional sponge of miR-486-5p and that miR-486-5p directly regulated the expression level of downstream EIF5A2. Likewise, miR-486-5p depletion attenuated the inhibitory effects of LINC00174 or EIF5A2 knockdown on OSCC cell malignancy due to their targeting relationship.

Conclusion LINC00174 is a driving factor in OSCC development by sponging miR-486-5p to regulate EIF5A2 expression. The LINC00174/miR-486-5p/EIF5A2 axis in OSCC, which is revealed in this study, may provide a new molecular network for understanding OSCC pathogenesis.

Keywords LINC00174 · miR-486-5p · EIF5A2 · Oral squamous cell carcinoma

Introduction

Oral squamous cell carcinoma (OSCC) is the most frequent cancer of the head and neck. OSCC accounts for approximately 2% of all malignancies worldwide and 1.8% of cancer-related deaths (Sung et al. 2021). Disease development is characterized by rapid proliferation, vascularization, and distant metastases (Jiang et al. 2020). Although the basic treatments for OSCC, including surgical resection supplemented by radiotherapy and chemotherapy, have been well developed to date (Gharat et al. 2016), the 5-year survival rate is only 50% (Ingaleshwar et al. 2016). Therefore, the complex molecular processes underlying OSCC progression remain to be fully understood.

Long non-coding RNAs (lncRNAs), which harbor more than 200 nucleotides, are regarded as important modulators of tumorigenesis through their effects on tumor cell behaviors, such as proliferation, invasion, and programmed death (Jiang et al. 2021; Peng et al. 2017; Sun and Ye 2020). In OSCC, lncRNA TUG1 serves as a competing endogenous RNA (ceRNA) that competes with DLX1 for miR-524-5p, thereby enhancing the proliferative and migratory ability of OSCC cells (Liu et al. 2019b). LINC00319 is highly expressed in OSCC, and downregulation of its expression significantly inhibits angiogenesis, epithelial–mesenchymal transition (EMT), and the proliferation of OSCC cells (Jiang

Xiao Feng and Jia Tu contribute equally to this work.

✉ Yan Guan
yanguan77@163.com

[1] Department of Stomatology, Hubei Provincial Hospital of Traditional Chinese Medicine, No. 856, Luoyu Road, Hongshan District, Wuhan 430061, Hubei, China

Published online: 22 December 2023

et al. 2020). Although the significance of a large number of lncRNAs in OSCC has been functionally characterized, the function of many differentially expressed lncRNAs in OSCC is still unknown. LINC00174 is a key regulator in multiple cancers (Cheng et al. 2022; Li et al. 2022; Zhao et al. 2020). LINC00174 acts as a driving factor to promote the progression of glioma and thymic epithelial tumors (Shi et al. 2019; Tito et al. 2020). However, the expression of LINC00174 is reduced in non-small cell lung cancer and its overexpression suppresses tumorigenesis (Cheng et al. 2022). To date, no studies have revealed the function of LINC00174 in OSCC.

LncRNAs have been widely recognized to act as ceRNAs to regulate microRNAs (miRNAs), thereby participating in tumorigenesis (Guo et al. 2021; Kong et al. 2019; Wang et al. 2019). miR-486-5p is a well-studied tumor suppressor in many malignancies (He et al. 2019; Tian et al. 2019; Zhang et al. 2016). According to a previous study, miR-486-5p, which is regulated by LINC01194, attenuates the malignancy of non-small cell lung cancer (Xing et al. 2020). miR-486-5p can also be sponged by lncRNA XIST to play an inhibitory role in colorectal cancer (Liu et al. 2019a). In OSCC, miR-486-5p expression has only been reported to be reduced in salivary exosomes of patients (Faur et al. 2022). However, the specific regulatory mechanism and function of miR-486-5p in OSCC are still unknown.

Eukaryotic initiation factor-5A2 (EIF5A2), located on human chromosome 3q26, is an oncogene in multiple cancers (Guan et al. 2001; Zhao et al. 2021; Zhong et al. 2020). Accumulating evidence has revealed that EIF5A2 can enhance xenograft tumor growth, promote cancer cell metastasis, and induce chemotherapeutic drug resistance (Tang et al. 2010; Yang et al. 2015; Zhu et al. 2012). EIF5A2 overexpression has been associated with unfavorable 5-year survival rate, advanced N values, and the presence of EMT markers in 272 patients with OSCC (Lin et al. 2020). Therefore, we believe that regulating EIF5A2 expression may affect the progression of OSCC; this needs further validation.

The goal of the present study was to confirm LINC00174 expression patterns and function in OSCC. Our findings enrich the understanding of lncRNA regulatory mechanisms in OSCC progression and provide a potential biomarker for OSCC treatment.

Materials and methods

Tissue samples

The Hubei Provincial Hospital of Traditional Chinese Medicine Institutional Review Board approved this study (approval number: HBZY2022-C34-07). All procedures involving the use of human samples were performed in accordance with the Declaration of Helsinki. A total of 38 OSCC tumor samples and paired non-cancerous normal samples were surgically removed from patients with OSCC at our hospital. Written informed consent was supplied by each patient. Following resection, tissue samples were instantly frozen in liquid nitrogen and kept in freezers at − 80 °C. Table 1 lists the characteristics of 38 patients with OSCC.

Cell culture and transfections

We purchased OSCC cells (SCC-4, SCC-9, and Cal-27) and non-cancerous oral cells (HIOEC) from BeNa Co., Ltd. (Beijing, China). The SCC-9 cells were cultivated with RPMI 1640 (BeNa Co., Ltd) supplemented with 10% FBS (BeNa Co., Ltd), and the HIOEC and SCC-4 and Cal-27 cells were cultivated in DMEM (BeNa Co., Ltd) supplemented with 10% FBS, in a 37 °C incubator containing 5% CO_2.

GeneChem (Shanghai, China) created and distributed small-interfering RNAs against LINC00174 (si-LINC00174) or EIF5A2 (si-EIF5A2) as well as a matching negative controls (si-NC). The LINC00174 overexpression vector (lnc-OE) was provided by GeneChem using pcDNA3.1, and a pcDNA3.1 empty vector was used as negative control (NC-OE). miR-486-5p mimics (miR-486-5p), miR-486-5p inhibitors (inhibitor), and matched negative controls (miR-NC and inhibitor-NC) were purchased from RiboBio (Guangzhou, China). For cell transfection, 50 nM si-LINC00174, 50 nM

Table 1 Clinicopathologic features of patients (N = 38)

Characteristics	No. of patients	No. %
Age (years)		
≥ 60	25	65.79
	13	34.21
Gender		
Male	31	81.58
Female	7	18.42
Tumor size (cm)		
≤ 2	30	78.95
2	8	21.05
TNM stage		
I	12	31.58
II	11	28.95
III	8	21.05
IV	7	18.42
Differentiation		
Well	24	63.16
Moderately/poorly	14	36.84
Local invasion		
No	29	76.32
Yes	9	23.68

si-EIF5A2, 75 nM miR-486-5p, 75 nM inhibitor, and their matched negative controls (50 nM si-NC, 75 nM miR-NC, and 75 nM inhibitor-NC) were transfected into SCC-4 and SCC-9 cells using Lipofectamine 3000 (Invitrogen, Carlsbad, CA, USA). After transfection, the cells were cultured for 48 h and then collected for detection of transfection efficiency using RT-qPCR or western blot.

RT-qPCR

A commercial TRIzol reagent (Invitrogen) was used to obtain total RNA. Subsequent reverse transcription of RNA was conducted using the QuantiTect Reverse Transcription Kit (Qiagen, Duesseldorf, Germany) or the miRNA Reverse Transcription Kit specific to miRNAs (Qiagen). The diluted cDNA was detected using qPCR with the use of SYBR Premix Ex Taq II (Takara, Dalian, China) according to the protocol guidelines (95 °C for 30 s followed by 40 cycles of 90 °C for 5 s and 60 °C for 30 s) on a LightCycler 96 thermocycler (Roche, Basel, Switzerland). GAPDH (for lncRNA and mRNA) or U6 (for miRNA) were used as the internal reference. The Ct values were processed using the $2^{-\Delta\Delta Ct}$ method. The primers used are presented in Table 2.

Subcellular localization assay

Using a PARIS kit (Invitrogen), cytoplasmic and nuclear RNA were extracted from SCC-4 and SCC-9 cells, respectively, to determine whether LINC00174 is localized in the cytoplasm or nucleus. Briefly, 500 µL ice-cold cell disruption buffer was added to 1×10^6 cells followed by incubation on ice for 5 min. After centrifugation at 500×*g*, the cell supernatant containing the cytoplasmic fraction and the pellet containing the nuclear fraction were collected. Finally, total RNA was isolated from the cytoplasm and nucleus, and northern blotting was performed to confirm LINC00174 localization.

Table 2 Real-time PCR primer synthesis list

Gene	Sequences	
LINC00174	Forward	5′-AATTCCTGTCTCCCGTTGGC-3′
	Reverse	5′-GGAGCTGGGCAGAAGAGTTT-3′
miR-486-5p	Forward	5′-CTCGCTTCGGCAGCACA-3′
	Reverse	5′-ACGCTTCACGAATTTGCGT-3′
EIF5A2	Forward	5′-CTTTCAGCCTGTGTAGGGCA-3′
	Reverse	5′-GTTGCATGTGGCCACCAAAA-3′
U6	Forward	5′-CTCGCTTCGGCAGCACA-3′
	Reverse	5′-AACGCTTCACGAATTTGCGT-3′
GAPDH	Forward	5′-AGAAAAACCTGCCAAATATGATGAC-3′
	Reverse	5′-TGGGTGTCGCTGTTGAAGTC-3′

CCK-8 assay

The transfected cells were seeded into 96-well plates (5×10^3 cells/well) and cultured at a 37 °C environment with 5% CO_2. Cells in different wells were administered 10 µL CCK-8 solution (Beyotime, Shanghai, China) at 0, 24, 48, and 72 h. After treating the cells with CCK-8 for 2 h, the absorbance at 450 nm was measured in different wells using a microplate reader (BioTek, USA).

Colony formation assay

The transfected cells were plated into 6-well plates (300 cells/well) and maintained at a 37 °C environment with 5% CO_2. The cell medium was refreshed every three days. After maintaining the cells for 14 days, cell colonies (> 50 cells) were immobilized using 4% paraformaldehyde (Beyotime) and stained using 0.5% crystal violet (Beyotime). Finally, the colonies were photographed under an inverted microscope (Olympus, Tokyo, Japan).

Wound healing (scratch) assay

Confluent monolayers of cells were cultivated in 24-well plates until they reached > 90% confluence. A simulated wound was generated in the monolayer with a 200-µL pipette tip. Serum-free medium was used to sustain the cells for 24 h. The extent of wound healing was photographed under an inverted microscope (Olympus) at the 0 and 24 h time points.

Xenograft models

The animal studies were approved by the Ethics Committee of the Hubei Provincial Hospital of Traditional Chinese Medicine (approval number: 202205019). Female BALB/c nude mice (Vital River, Beijing, China) were housed in an animal room without pathogens. To create subcutaneous tumor models, SCC-4 cells were suspended in 100 µL of phosphate-buffered saline (PBS) and then injected into mice (2×10^6 cells/mouse; n = 5 per group) after infection with lentivirus-packaged sh-lnc (short-hairpin-RNA targeting LINC00174; Geneseed, Guangzhou, China) or sh-NC. Tumor volume (length × width^2 × 0.5) was documented every week. At 5 weeks post-injection, the animals were euthanized and the tumor tissues were harvested.

Dual-luciferase assay

As the WT reporter vector of LINC00174 or EIF5A2, a sequence segment of the 3′UTR of LINC00174 or EIF5A2 that included miR-486-5p binding sites was created and inserted into the pmirGLO vector (Promega, Madison, WI,

USA), downstream of the luciferase reporter gene. The MUT reporter vector of LINC00174 or EIF5A2 was also created using a sequence segment of the 3′UTR of LINC00174 or EIF5A2 that featured site-directed mutagenesis of the anticipated miR-486-5p binding sites using the QuickMutation Site-Directed Mutagenesis Kit (Beyotime). The WT or MUT vector of LINC00174 or EIF5A2 was co-transfected with miR-486-5p or miR-NC into OSCC cells. The Dual-Luciferase Reporter Assay System (Promega) was used to measure luciferase activity after 48 h of cell maintenance.

RIP assay

A commercial RIP Assay Kit (Millipore, Billerica, MA, USA) was used to investigate if Ago2 interfered with the binding of miR-486-5p to LINC00174. In brief, 200 µL RIP lysis buffer was added to SCC-4 and SCC-9 cells, which were then incubated for 5 min on ice. The lysates of SCC-4 and SCC-9 cells were then collected using centrifugation at 500×*g* for 5 min and incubated with magnetic beads pretreated with anti-IgG (negative control) or anti-Ago2 overnight at 4 °C. Next, the RNA samples were isolated from the beads, and the levels of LINC00174 and miR-486-5p were examined using RT-qPCR.

Western blot

RIPA buffer (Beyotime) was used to pull out the proteins, a BCA kit (Beyotime) to measure protein concentration, and 10% SDS-PAGE to separate the proteins. The purified protein bands were deposited on PVDF membranes (0.22 µm thickness) and the membranes were then blocked with 5% non-fat milk at room temperature for 1 h. Next, the membranes were incubated with primary antibodies against GAPDH (ab9485; 1/2500; Abcam, Cambridge, MA, USA) or EIF5A2 (ab227537; 1/1000; Abcam). ECL reagent (Beyotime) was used to identify the protein signals on the membranes after incubation with HRP-conjugated secondary antibodies (ab205718; 1/20000; Abcam).

Statistical analysis

Using GraphPad Prism 8.0 (GraphPad, USA), the data from three separate trials were collected and analyzed. The means and standard deviations of the results are shown. The Student's *t* test was used for comparisons involving two sets of data, whereas analysis of variance was used for comparisons involving several groups. Fisher's exact test was used to analyze the correlation between LINC00174 expression and clinical characteristics. The Pearson's correlation test was used to assess expression correlation. Differences at $P < 0.05$ were deemed statistically significant.

Results

LINC00174 with high expression in OSCC

After collecting OSCC and adjacent normal tissues from 38 patients with OSCC, we used RT-qPCR to assess LINC00174 expression. The results showed that LINC00174 expression was upregulated by 6.3-fold in the OSCC samples compared to the normal samples (Fig. 1A). Statistical analysis using Fisher's exact test showed that LINC00174 expression correlated with TNM stage, differentiation, and local invasion (Table 3). RT-qPCR revealed that LINC00174 expression was significantly enhanced in SCC-9, Cal-27, and SCC-4 cells compared to that in HIOEC (Fig. 1B). Due to the higher LINC00174 expression in SCC-4 and SCC-9 cells, we selected SCC-4 and SCC-9 cells as representative OSCC cell lines for subsequent experiments. The subcellular localization assay confirmed that LINC00174 was primarily localized in the cytoplasmic fraction of SCC-4 and SCC-9 cells rather than in the nucleus (Fig. 1C). These data confirm that LINC00174, localized in the cytoplasm, exhibits upregulated expression in OSCC.

LINC00174 absence blocked OSCC cell growth and migration

In view of the overexpression of LINC00174 in OSCC, we depleted LINC00174 expression in OSCC cells to explore its function by transfecting cells with si-LINC00174 (si-lnc). RT-qPCR analysis showed that LINC00174 expression was reduced by 70% in the SCC-4 and SCC-9 cells after si-lnc transfection (Fig. 2A). The CCK-8 assay verified that the proliferative ability of OSCC cells in the absence of LINC00174 was markedly repressed (Fig. 2B). The colony formation assay further confirmed that LINC00174 silencing resulted in a decreased number of OSCC colonies (Fig. 2C). In addition, the rate of migration of OSCC cells was notably reduced after si-lnc transfection, implying that LINC00174 absence markedly restrained cell migration (Fig. 2D). In short, LINC00174 absence restrains OSCC cell malignancy in vitro.

LINC00174 expression depletion hindered tumor development in vivo

To explore the effect of LINC00174 on OSCC development in vivo, we inoculated nude mice (2×10^6 cells per mouse, n = 5 per group) with sh-LINC00174 (sh-lnc) or sh-NC-infected SCC-4 cells. Consequently, we found that tumor size in the sh-lnc-administered animals was noticeably smaller than that in the sh-NC-administered animals

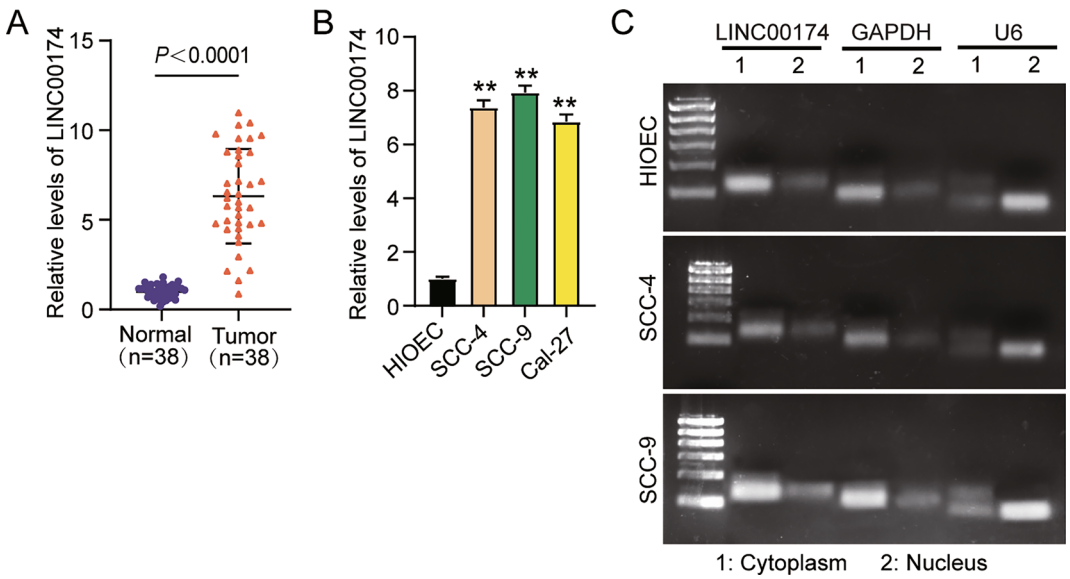

Fig. 1 LINC00174 was overexpressed in OSCC. **A** The expression of LINC00174 in OSCC tumor tissues and normal samples was examined using RT-PCR. **B** LINC00174 expression in HIOEC and OSCC cells (Cal-27, SCC-4, and SCC-9) was evaluated using RT-PCR; $^{**}P < 0.01$ versus HIOEC. **C** Subcellular localization of LINC00174 in the cytoplasm and nucleus of OSCC cells. All data derived from three independent experiments

Table 3 The correlation between LINC00174 expression and characteristics of patients

Characteristics	LINC00174 expression		*P* value
	High (n = 18)	Low (n = 20)	
Age (years)			0.5064
≥ 60	13	12	
< 60	5	8	
Gender			0.6867
Male	14	17	
Female	4	3	
Tumor size (cm)			0.1171
≤ 2	12	18	
> 2	6	2	
TNM stage			0.0004
I	1	11	
II	4	7	
III	6	2	
IV	7	0	
Differentiation			0.0424
Well	8	16	
Moderately/poorly	10	4	
Local invasion			0.0067
No	10	19	
Yes	8	1	

Fisher's exact test was used to perform statistical analysis

(Fig. 3A). In addition, the tumor volume and weight from the mice in the sh-lnc group noticeably decreased (Fig. 3B, C). These results demonstrate that LINC00174 depletion impedes tumor growth in vivo.

LINC00174 may act as a functional sponge of miR-486-5p

The starBase website predicted that LINC00174 possessed putative binding sites for miR-486-5p (Fig. 4A). The dual-luciferase assay showed that luciferase activity was reduced (by approximately 50%) only in OSCC cells co-transfected with the miR-486-5p mimic and wild-type vector of LINC00174, suggesting the presence of binding sites between LINC00174 and miR-486-5p (Fig. 4B). The substantial enrichment of LINC00174 as well as miR-486-5p by anti-Ago2 in the RIP assay serves as evidence that Ago2 primarily mediates the binding of LINC00174 to miR-486-5p (Fig. 4C). In our collected clinical samples, compared to normal samples, miR-486-5p expression levels in OSCC tissues were reduced by 53% (Fig. 4D). miR-486-5p expression levels also decreased by > 50% in SCC-4 and SCC-9 cells, compared to those in HIOEC (Fig. 4E). Pearson's correlation test showed that the level of miR-486-5p expression in the OSCC samples inversely correlated with LINC00174 expression (Fig. 4F). After transfecting LINC00174 overexpression vectors into SCC-4 and SCC-9 cells, miR-486-5p expression was downregulated by > 50% (Fig. 4G). Overall, these results demonstrate that LINC00174 directly targets miR-486-5p.

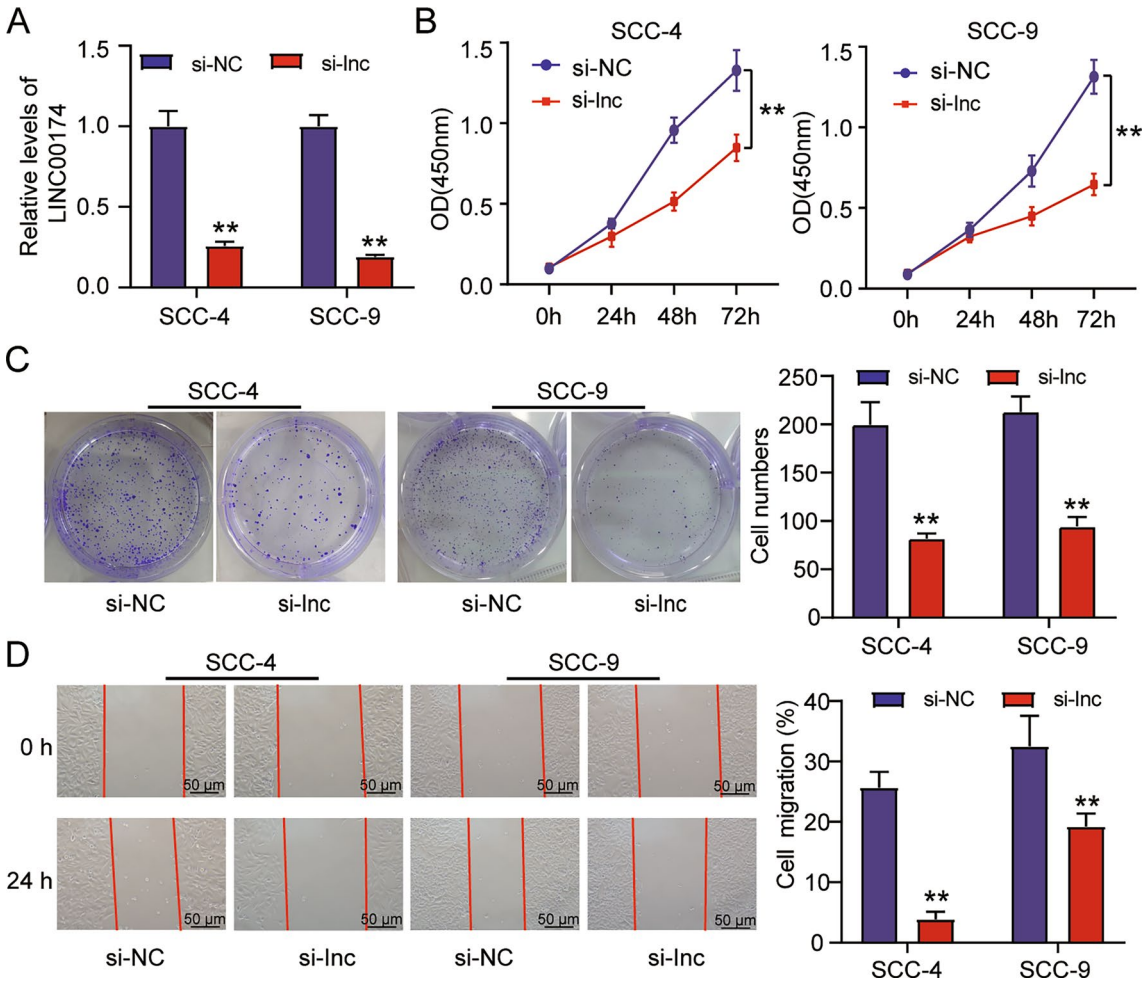

Fig. 2 LINC00174 absence restrained OSCC cell growth and migration. **A** The siRNA-mediated inhibitory effect of LINC00174 on SCC-4 and SCC-9 cells was assessed using RT-PCR. **B** The effect of LINC00174 absence on cell proliferation was assessed using the CCK-8 test. **C** The effect of LINC00174 absence on colony formation was assessed using a colony formation test. **D** The effect of LINC00174 absence on migration was assessed using a wound healing experiment. $^{**}P < 0.01$ versus si-NC. All data derived from three independent experiments

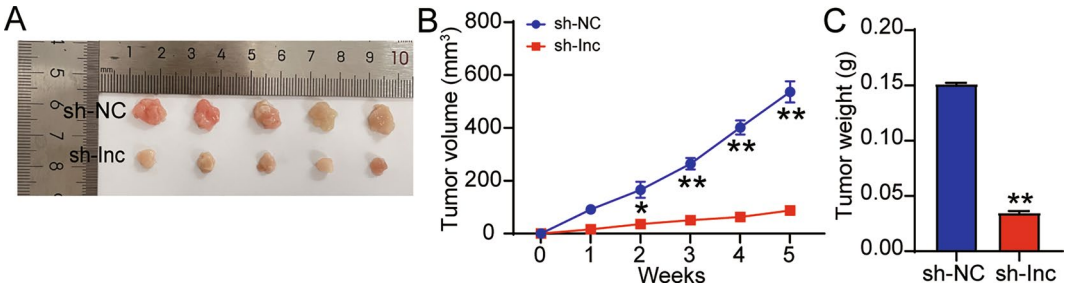

Fig. 3 LINC00174 deficiency restrained OSCC tumor growth in mouse models. **A**–**C** SCC-4 cells infected with lentivirus-packaged sh-LINC00174 (sh-lnc) or sh-NC in 100 μL PBS were injected into mice (2×10^6 cells/mouse; n = 5 per group). **A** Tumor tissues collected from mice. **B** Tumor volumes were measured weekly to assess tumor development. $^{**}P < 0.01$ versus sh-NC. **C** Tumor weights were investigated after housing the mice for 5 weeks to assess tumor development. $^{**}P < 0.01$ versus sh-NC. All data derived from three independent experiments

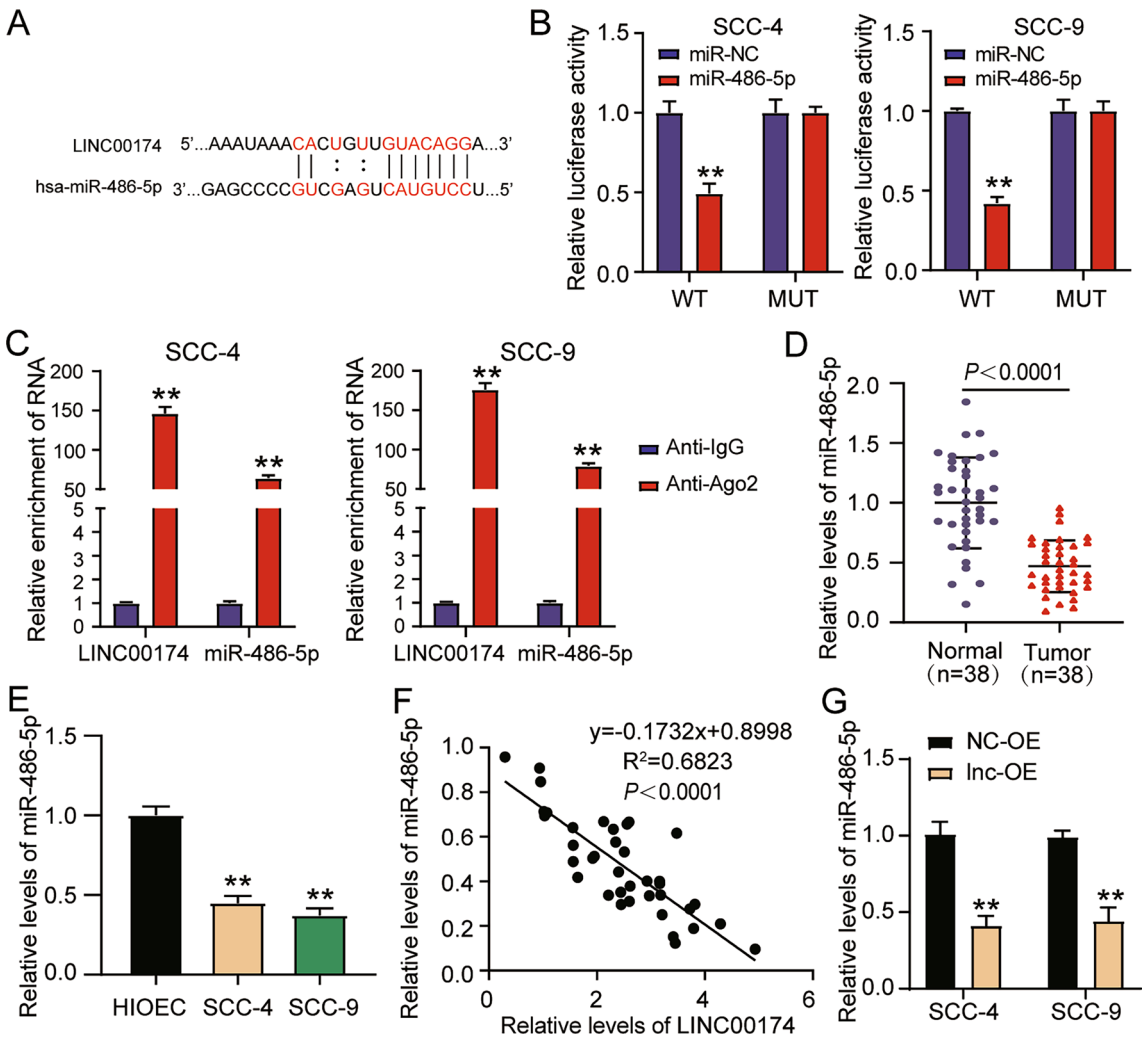

Fig. 4 LINC00174 targeted miR-486-5p. **A** LINC00174 binding to miR-486-5p was predicted using starBase. **B** The predicted binding sites among LINC00174 and miR-486-5p were validated using dual-luciferase assays; $^{**}P<0.01$ versus miR-NC. **C** The miR-486-5p connection to LINC00174 was confirmed using RIP assays; $^{**}P<0.01$ versus anti-IgG. **D** The miR-486-5p expression in tumor and normal samples was evaluated via RT-qPCR. **E** RT-PCR was used to evaluate the expression of miR-486-5p in OSCC cells (SCC-4 and SCC-9) and HIOEC, $^{**}P<0.01$ versus HIOEC. **F** The relationship between the expression levels of miR-486-5p and LINC00174 in tumor tissues were assessed using the Pearson correlation test. **G** The miR-486-5p expression in SCC-4 and SCC-9 cells transfected with LINC00174 overexpression vectors was evaluated via RT-qPCR. $^{**}P<0.01$ versus NC-OE. All data derived from three independent experiments

LINC00174 absence reinforced miR-486-5p expression and thus produced cancer-suppressive effects in OSCC

After transfecting OSCC cells with si-lnc and miR-486-5p inhibitor, we detected that miR-486-5p levels were exceptionally strengthened by the si-lnc transfection but depleted by the transfection of the miR-486-5p inhibitor (Fig. 5A). We then characterized the inhibitory role of miR-486-5p and the effects of miR-486-5p on si-lnc-regulated OSCC cell functions. miR-486-5p inhibition considerably strengthened the proliferative, colony formation, and migratory capacity of the SCC-4 and SCC-9 cells (Fig. 5B–D). Interestingly, the promoting effects of the miR-486-5p inhibitor on OSCC cell processes were partially abolished by LINC00174 absence; the effect was evidenced by the promotion of proliferation, migration, and colony formation in si-lnc + inhibitor-transfected OSCC cells compared with si-lnc-transfected cells (Fig. 5B–D). These results suggest that LINC00174 absence represses OSCC cell functions via upregulation of miR-486-5p expression.

miR-486-5p targeted EIF5A2

The frequently used bioinformatics tool TargetScan was applied to determine the targets of miR-486-5p. miR-486-5p

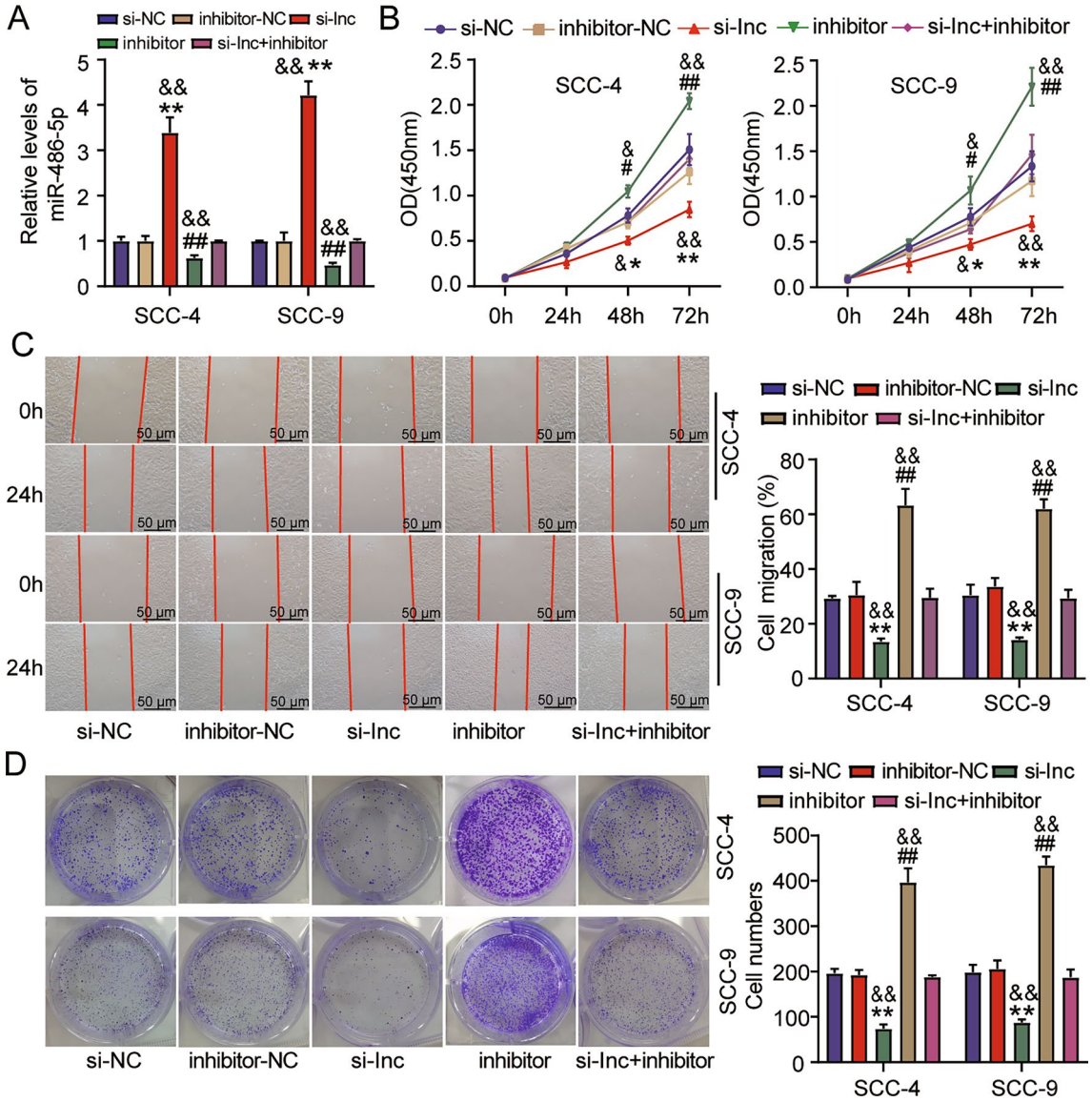

Fig. 5 LINC00174 absence restrained OSCC cell growth and migration by upregulating miR-486-5p expression. **A** miR-486-5p expression levels in SCC-4 and SCC-9 cells transfected with si-NC, inhibitor-NC, si-lnc, inhibitor, or si-lnc + inhibitor. **B** CCK-8 assay was conducted using these transfected cells to evaluate proliferation capacity. **C** These transfected cells were used in a wound healing test to quantify migration ability. **D** Capacity for colony formation. $^{*}P<0.05$ and $^{**}P<0.01$ versus si-NC; $^{\#}P<0.05$ and $^{\#\#}P<0.01$ versus inhibitor-NC; $^{\&}P<0.05$ and $^{\&\&}P<0.01$ versus si-lnc + inhibitor. All data derived from three independent experiments

was displayed to harbor binding sites on EIF5A2 3′UTR (Fig. 6A). Luciferase activity in SCC-4 and SCC-9 cells co-transfected with miR-486-5p mimic and EIF5A2 wild-type vector was reduced, verifying the presence of binding sites between miR-486-5p and EIF5A2 (Fig. 6B). RT-qPCR analysis showed that the EIF5A2 mRNA expression increased greatly in the OSCC compared to the normal samples, and in SCC-4 and SCC-9 cells compared to HIOEC (Fig. 6C–D). miR-486-5p expression in OSCC samples was passively associated with EIF5A2 expression (Fig. 6E). Western blot analysis showed that LINC00174 knockdown reduced EIF5A2 expression, while the miR-486-5p inhibitor elevated EIF5A2 expression (Fig. 6F). These data indicate that miR-486-5p targets EIF5A2.

miR-486-5p inhibition strengthened EIF5A2 expression and thus attenuated the cancer-suppressive effects of EIF5A2 knockdown in OSCC

After transfecting si-EIF5A2 and the miR-486-5p inhibitor into OSCC cells, western blot assay showed that the

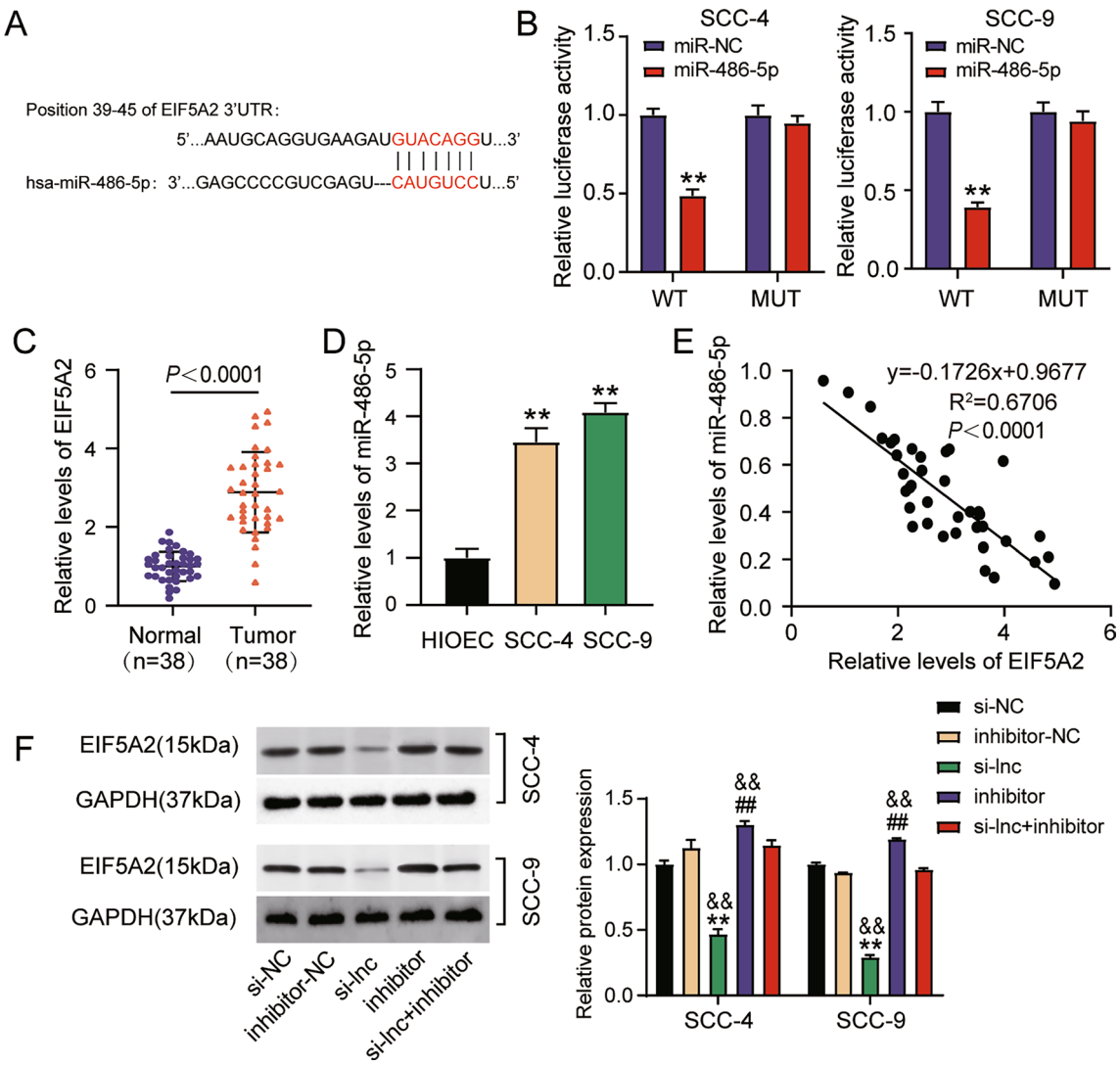

Fig. 6 miR-486-5p bound to EIF5A2. **A** The binding sites for miR-486-5p on the 3′UTR of EIF5A2 were ascertained using TargetScan data. **B** The anticipated binding of miR-486-5p to EIF5A2 was confirmed using dual-luciferase assays; $^{**}P<0.01$ versus miR-NC. **C** The EIF5A2 mRNA expression level in tumor and normal samples was evaluated using RT-PCR. **D** The mRNA expression level of EIF5A2 in HIOEC and OSCC cells (SCC-9 and SCC-4) was evaluated using RT-PCR, $^{**}P<0.01$ versus HIOEC. **E** Pearson correlation was used to examine the relationship between the expression levels of miR-486-5p and EIF5A2 in tumor samples. **F** EIF5A2 protein expression in SCC-4 and SCC-9 cells transfected with si-NC, inhibitor-NC, si-lnc, inhibitor, or si-lnc + inhibitor was detected using western blot. $^{\&\&}P<0.01$ versus si-lnc + inhibitor; $^{**}P<0.01$ versus si-NC; $^{\#\#}P<0.01$ versus inhibitor-NC. All data derived from three independent experiments

expression of the EIF5A2 protein was greatly impaired by si-EIF5A2 transfection but strengthened by transfection with the miR-486-5p inhibitor (Fig. 7A). Regarding functions, EIF5A2 knockdown considerably obstructed SCC-4 and SCC-9 cell proliferative, migratory, and colony formation abilities (Fig. 7B–D). However, the suppressive effects of EIF5A2 silencing were largely attenuated by miR-486-5p inhibition, evidenced by the promotion of proliferation, migration, and colony formation in si-EIF5A2 + inhibitor-transfected cells compared to si-EIF5A2-transfected cells (Fig. 7B–D). These data manifest that miR-486-5p governs EIF5A2 expression to regulate OSCC cell functions.

Discussion

Our current study reported that LINC00174 expression is upregulated in OSCC and correlates with TNM stage, differentiation, and local invasion. Silencing LINC00174 in OSCC cells led to the inhibition of cell growth and migration in vitro and in vivo. Mechanically, we determined

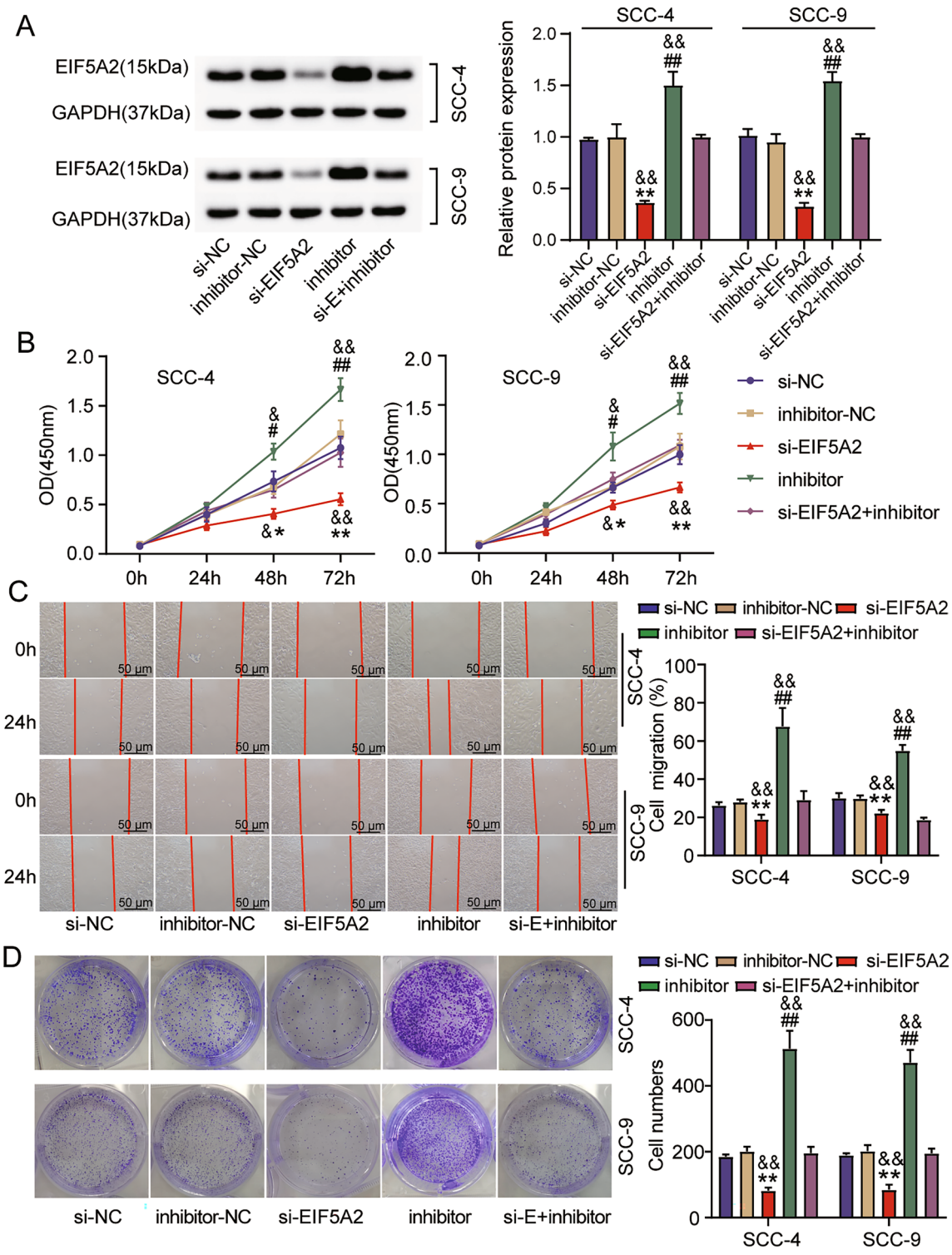

Fig. 7 miR-486-5p inhibition promoted EIF5A2 expression and thus attenuated the anti-cancer effects of EIF5A2 knockdown. **A** EIF5A2 protein expression in SCC-4 and SCC-9 cells transfected with si-NC, inhibitor-NC, si-EIF5A2, inhibitor, or si-EIF5A2 + inhibitor. **B** A CCK-8 assay was performed using these cells to observe proliferation. **C** A wound healing assay was executed employing these cells to observe migration. **D** These cells were used in a colony formation experiment. $^{\&}P < 0.05$ and $^{\&\&}P < 0.01$ versus si-EIF5A2 + inhibitor; $^{*}P < 0.05$ and $^{**}P < 0.01$ versus si-NC; $^{\#}P < 0.05$ and $^{\#\#}P < 0.01$ versus inhibitor-NC. All data were from three independent experiments

that LINC00174 targeted miR-486-5p and controlled miR-486-5p expression, thereby regulating the targeted gene EIF5A2 of miR-486-5p. The findings of this study reveal that LINC00174 enhances OSCC malignancy by sponging miR-486-5p to upregulate EIF5A2 expression (Fig. 8).

The functional role of LINC00174 in several cancers has been established. For example, LINC00174 shows an elevated expression pattern in colorectal cancer, and silencing of LINC00174 represses cell growth, solid tumor growth, and temozolomide chemoresistance (Li et al. 2020; Shen et al. 2018). LINC00174 is overexpressed in glioma and its deficiency impairs glioma cell growth, survival, motility, and glycolysis metabolism (Shi et al. 2019). Aberrantly high expression of LINC00174 has also been identified in osteosarcoma, where LINC00174 downregulation blocks cell growth, migration, and tumorigenesis (Zheng et al. 2021). However, in non-small cell lung cancer, LINC00174 expression is downregulated, indicating that LINC00174 plays an inhibitory role in tumorigenesis (Cheng et al. 2022). The previous studies suggest that LINC00174 plays different roles in different cancer types. Regarding OSCC, the function of LINC00174 is still not elucidated. This study is the first to confirm the elevated expression of LINC00174 in OSCC, and that silencing LINC00174 restrained OSCC cell proliferative, migratory, and colony formation abilities in vitro and tumor development in vivo. Furthermore, in clinical samples from 38 patients with OSCC, we demonstrated that LINC00174 expression correlated with TNM stage, differentiation, and local invasion. Therefore, our results clearly indicate that targeting LINC00174 may help relieve tumorigenesis in OSCC.

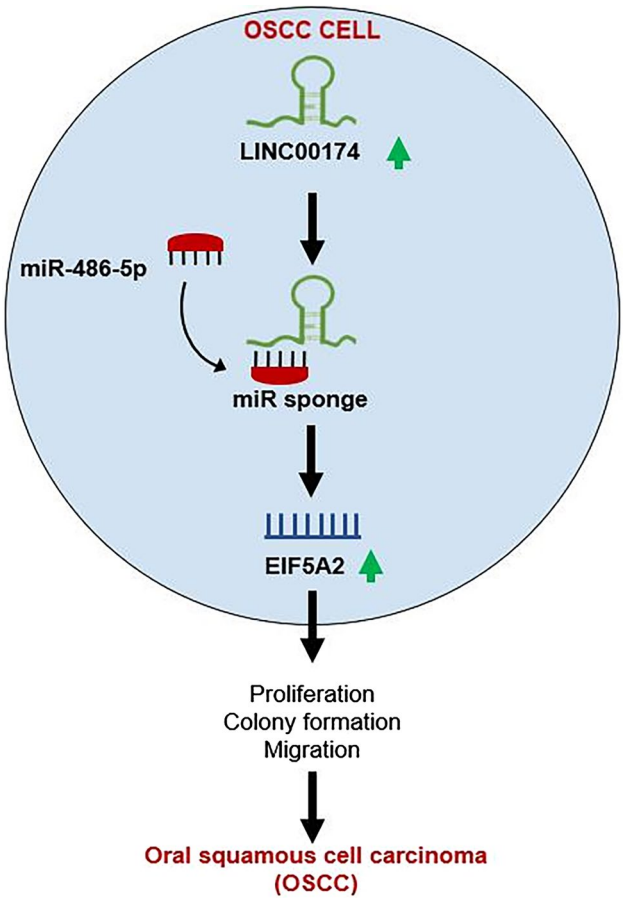

Fig. 8 The mechanism of action of the LINC00174/miR-486-5p/EIF5A2 axis in OSCC

Previous evidence suggests that LINC00174 can disturb miRNA pathways by binding miRNA response elements, and that these interactions are involved in the progression of various cancers (Li et al. 2020; Shen et al. 2018; Shi et al. 2019). Using the starBase database, dual-luciferase, and RIP assays, we demonstrated that miR-486-5p binds to LINC00174. Previous studies have revealed that miR-486-5p plays an inhibitory role in multiple cancers by binding to different lncRNAs. For example, in colorectal cancer, miR-486-5p binds to lncRNA NEAT1, thereby acting as a tumor suppressor (Liu et al. 2021). miR-486-5p, sponged by lncRNA LINC01194, attenuates cell proliferation and migration in non-small cell lung cancer (Xing et al. 2020). Regarding OSCC, in 2017, Yan et al. firstly used next-generation sequencing technology to confirm that miR-486-5p expression is downregulated in OSCC samples, and that its downregulation is associated with OSCC recurrence (Yan et al. 2017). In 2022, Faur et al. found that miR-486-5p is only reduced in salivary exosomes from patients with OSCC (Faur et al. 2022). Although the earlier studies have not explored the specific function of miR-486-5p in OSCC, the downregulation of miR-486-5p expression in this cancer has been confirmed, suggesting a key role in OSCC development. Here, we investigated in depth the function of miR-486-5p and revealed that an miR-486-5p inhibitor aggravated OSCC cell proliferative, migratory, and colony formation abilities. Moreover, we confirmed that EIF5A2 is a target gene of miR-486-5p in OSCC.

EIF5A2 is a well-recognized oncogene that contributes to proliferation, invasion, metastasis, and other aggressive behaviors in various cancer cells (Ba et al. 2019; Zhao et al. 2021; Zheng et al. 2020). High expression of EIF5A2 is linked to poor outcomes in patients with gallbladder and cervical cancer, as well as OSCC (Lin et al. 2020; Yang et al. 2016; Zheng et al. 2020). Furthermore, high expression of EIF5A2 is associated with unfavorable 5-year survival rates, advanced N values, and EMT markers in 272 patients with OSCC (Lin et al. 2020). In vitro, Gao et al. used the OSCC cell line SCC-9 to show that EIF2A knockdown inhibits migration and invasion (Gao and Li 2023). Consistent with previous studies, this study, too, demonstrated overexpression of EIF5A2 in OSCC, and that EIF5A2 silencing is linked to the inhibition of cancer cell growth and migration. However, a novel finding was

that miR-486-5p depletion attenuated the inhibitory effects of EIF5A2 silencing on OSCC cell development because EIF5A2 is a target gene of miR-486-5p.

This study proposes a new regulatory network for LINC00174/miR-486-5p/EIF5A2 in OSCC progression. However, some limitations are noted. First, this study did not explore the possible relationship between LINC00174 and prognosis of patients with OSCC because of the small clinical sample size and absence of long-term follow-up for all included patients. In addition, the regulatory mechanism of lncRNA in OSCC development is complex, and other potential oncogenic signaling pathways involved in LINC00174-governed networks should be further explored in the future.

In conclusion, this study revealed that LINC00174 was aberrantly upregulated in OSCC, and that silencing LINC00174 attenuated OSCC malignancy by sponging miR-486-5p to regulate EIF5A2 expression. These findings enrich our understanding of the regulatory network of lncRNAs in OSCC progression and may provide a novel biomarker for OSCC diagnosis and therapy.

Acknowledgements None.

Author contributions The tests were run, and the data was analyzed by XF and YG. The study was created and produced by JT. The data was acquired using XF. The data was analyzed and interpreted by JT and YG. The article was reviewed and approved by all writers.

Funding This study did not receive any funding in any form.

Data and material accessibility The datasets generated during and/or analysed during the current study are available from the corresponding author on reasonable request.

Declarations

Conflict of interest Xiao Feng, Jia Tu, Yan Guan declare no conflicts of interest.

Ethical approval The Hubei Provincial Hospital of Traditional Chinese Medicine's ethics committee (Wuhan, China) accepted this study (Approval number: HBZY2022-C34-07). The ethical standards specified in the Declaration of Helsinki are followed while processing clinical tissue samples. A written informed consent form was filled out by each patient. This animal experiment was authorized by the Hubei Provincial Hospital of Traditional Chinese Medicine's ethics committee (Approval number: 202205019) and was done in accordance with the ARRIVE standards.

Consent to participate A written informed consent form was filled out by each patient.

Consent for publication Participants approved the publication of their names.

References

Ba MC, Ba Z, Cui SZ, Gong YF, Chen C, Lin KP, Wu YB, Tu YN (2019) Thermo-chemotherapy inhibits the proliferation and metastasis of gastric cancer cells via suppression of EIF5A2 expression. Onco Targets Ther 12:6275–6284

Cheng X, Sha M, Jiang W, Chen L, Song M (2022) LINC00174 suppresses non-small cell lung cancer progression by up-regulating LATS2 via sponging miR-31-5p. Cell J 24:140–147

Faur CI, Roman RC, Jurj A, Raduly L, Almășan O, Rotaru H, Chirilă M, Moldovan MA, Hedeșiu M, Dinu C (2022) Salivary exosomal microRNA-486-5p and microRNA-10b-5p in oral and oropharyngeal squamous cell carcinoma. Medicina (kaunas) 58:1478

Gao J, Li P (2023) Targeting eIF5A2 reduces invasion and reverses chemoresistance in SCC-9 cells in vitro. Histol Histopathol. https://doi.org/10.14670/HH-18-637

Gharat SA, Momin M, Bhavsar C (2016) Oral squamous cell carcinoma: current treatment strategies and nanotechnology-based approaches for prevention and therapy. Crit Rev Ther Drug Carrier Syst 33:363–400

Guan XY, Sham JS, Tang TC, Fang Y, Huo KK, Yang JM (2001) Isolation of a novel candidate oncogene within a frequently amplified region at 3q26 in ovarian cancer. Cancer Res 61:3806–3809

Guo K, Qian K, Shi Y, Sun T, Wang Z (2021) LncRNA-MIAT promotes thyroid cancer progression and function as ceRNA to target EZH2 by sponging miR-150-5p. Cell Death Dis 12:1097

He J, Xiao B, Li X, He Y, Li L, Sun Z (2019) MiR-486-5p suppresses proliferation and migration of hepatocellular carcinoma cells through downregulation of the E3 ubiquitin ligase CBL. Biomed Res Int 2019:2732057

Ingaleshwar PS, Pandit S, Desai D, Redder CP, Shetty AS, Mithun KM (2016) Immunohistochemical analysis of angiogenesis by CD34 and mast cells by toluidine blue in different grades of oral squamous cell carcinoma. J Oral Maxillofac Pathol 20:467–473

Jiang N, Zhang X, Gu X, Li X, Shang L (2021) Progress in understanding the role of lncRNA in programmed cell death. Cell Death Discov 7:30

Jiang X, Liu J, Li S, Jia B, Huang Z, Shen J, Luo H, Zhao J (2020) CCL18-induced LINC00319 promotes proliferation and metastasis in oral squamous cell carcinoma via the miR-199a-5p/FZD4 axis. Cell Death Dis 11:777

Kong X, Duan Y, Sang Y, Li Y, Zhang H, Liang Y, Liu Y, Zhang N, Yang Q (2019) LncRNA-CDC6 promotes breast cancer progression and function as ceRNA to target CDC6 by sponging microRNA-215. J Cell Physiol 234:9105–9117

Li B, Zhao H, Song J, Wang F, Chen M (2020) LINC00174 downregulation decreases chemoresistance to temozolomide in human glioma cells by regulating miR-138-5p/SOX9 axis. Hum Cell 33:159–174

Li X, Liu W, Tao W (2022) LINC00174 promotes cell proliferation and metastasis in renal clear cell carcinoma by regulating miR-612/FOXM1 axis. Immunopharmacol Immunotoxicol 44:746–756

Lin YM, Chen ML, Chen CL, Yeh CM, Sung WW (2020) Overexpression of EIF5A2 predicts poor prognosis in patients with oral squamous cell carcinoma. Diagnostics (basel) 10:436

Liu A, Liu L, Lu H (2019a) LncRNA XIST facilitates proliferation and epithelial-mesenchymal transition of colorectal cancer cells through targeting miR-486-5p and promoting neuropilin-2. J Cell Physiol 234:13747–13761

Liu S, Liu LH, Hu WW, Wang M (2019b) Long noncoding RNA TUG1 regulates the development of oral squamous cell carcinoma through sponging miR-524-5p to mediate DLX1 expression as a competitive endogenous RNA. J Cell Physiol 234:20206–20216

Liu Z, Gu Y, Cheng X, Jiang H, Huang Y, Zhang Y, Yu G, Cheng Y, Zhou L (2021) Upregulation lnc-NEAT1 contributes to colorectal

cancer progression through sponging miR-486-5p and activating NR4A1/Wnt/β-catenin pathway. Cancer Biomark 30:309–319
Peng WX, Koirala P, Mo YY (2017) LncRNA-mediated regulation of cell signaling in cancer. Oncogene 36:5661–5667
Shen Y, Gao X, Tan W, Xu T (2018) STAT1-mediated upregulation of lncRNA LINC00174 functions a ceRNA for miR-1910-3p to facilitate colorectal carcinoma progression through regulation of TAZ. Gene 666:64–71
Shi J, Zhang Y, Qin B, Wang Y, Zhu X (2019) Long non-coding RNA LINC00174 promotes glycolysis and tumor progression by regulating miR-152-3p/SLC2A1 axis in glioma. J Exp Clin Cancer Res 38:395
Sun DE, Ye SY (2020) Emerging roles of long noncoding RNA regulator of reprogramming in cancer treatment. Cancer Manag Res 12:6103–6112
Sung H, Ferlay J, Siegel RL, Laversanne M, Soerjomataram I, Jemal A, Bray F (2021) Global cancer statistics 2020: GLOBOCAN estimates of incidence and mortality worldwide for 36 cancers in 185 countries. CA Cancer J Clin 71:209–249
Tang DJ, Dong SS, Ma NF, Xie D, Chen L, Fu L, Lau SH, Li Y, Li Y, Guan XY (2010) Overexpression of eukaryotic initiation factor 5A2 enhances cell motility and promotes tumor metastasis in hepatocellular carcinoma. Hepatology 51:1255–1263
Tian F, Wang J, Ouyang T, Lu N, Lu J, Shen Y, Bai Y, Xie X, Ge Q (2019) MiR-486-5p serves as a good biomarker in nonsmall cell lung cancer and suppresses cell growth with the involvement of a target PIK3R1. Front Genet 10:688
Tito C, Ganci F, Sacconi A, Masciarelli S, Fontemaggi G, Pulito C, Gallo E, Laquintana V, Iaiza A, De Angelis L, Benedetti A, Cacciotti J, Miglietta S, Bellenghi M, Carè A, Fatica A, Diso D, Anile M, Petrozza V, Facciolo F, Alessandrini G, Pescarmona E, Venuta F, Marino M, Blandino G, Fazi F (2020) LINC00174 is a novel prognostic factor in thymic epithelial tumors involved in cell migration and lipid metabolism. Cell Death Dis 11:959
Wang L, Cho KB, Li Y, Tao G, Xie Z, Guo B (2019) Long noncoding RNA (lncRNA)-mediated competing endogenous RNA networks provide novel potential biomarkers and therapeutic targets for colorectal cancer. Int J Mol Sci 20:5758
Xing Z, Zhang Z, Gao Y, Zhang X, Kong X, Zhang J, Bai H (2020) The lncRNA LINC01194/miR-486-5p axis facilitates malignancy in non-small cell lung cancer via regulating CDK4. Onco Targets Ther 13:3151–3163
Yan Y, Wang X, Venø MT, Bakholdt V, Sørensen JA, Krogdahl A, Sun Z, Gao S, Kjems J (2017) Circulating miRNAs as biomarkers for oral squamous cell carcinoma recurrence in operated patients. Oncotarget 8:8206–8214
Yang H, Li XD, Zhou Y, Ban X, Zeng TT, Li L, Zhang BZ, Yun J, Xie D, Guan XY, Li Y (2015) Stemness and chemotherapeutic drug resistance induced by EIF5A2 overexpression in esophageal squamous cell carcinoma. Oncotarget 6:26079–26089
Yang SS, Gao Y, Wang DY, Xia BR, Liu YD, Qin Y, Ning XM, Li GY, Hao LX, Xiao M, Zhang YY (2016) Overexpression of eukaryotic initiation factor 5A2 (EIF5A2) is associated with cancer progression and poor prognosis in patients with early-stage cervical cancer. Histopathology 69:276–287
Zhang X, Zhang T, Yang K, Zhang M, Wang K (2016) miR-486-5p suppresses prostate cancer metastasis by targeting snail and regulating epithelial-mesenchymal transition. Onco Targets Ther 9:6909–6914
Zhao G, Zhang W, Dong P, Watari H, Guo Y, Pfeffer LM, Tigyi G, Yue J (2021) EIF5A2 controls ovarian tumor growth and metastasis by promoting epithelial to mesenchymal transition via the TGFβ pathway. Cell Biosci 11:70
Zhao JT, Chi BJ, Sun Y, Chi NN, Zhang XM, Sun JB, Chen Y, Xia Y (2020) LINC00174 is an oncogenic lncRNA of hepatocellular carcinoma and regulates miR-320/S100A10 axis. Cell Biochem Funct 38:859–869
Zheng C, Li R, Zheng S, Fang H, Xu M, Zhong L (2021) LINC00174 facilitates cell proliferation, cell migration and tumor growth of osteosarcoma via regulating the TGF-β/SMAD signaling pathway and upregulating SSH2 expression. Front Mol Biosci 8:697773
Zheng X, Gao L, Wang BT, Shen P, Yuan XF, Zhang LQ, Yang L, Zhang DP, Zhang Q, Wang XM (2020) Overexpression of EIF5A2 is associated with poor survival and aggressive tumor biology in gallbladder cancer. Histol Histopathol 35:579–587
Zhong X, Xiu H, Bi Y, Zhang H, Chang L, Diao H (2020) Targeting eIF5A2 inhibits prostate carcinogenesis, migration, invasion and metastasis in vitro and in vivo. Bioengineered 11:619–627
Zhu W, Cai MY, Tong ZT, Dong SS, Mai SJ, Liao YJ, Bian XW, Lin MC, Kung HF, Zeng YX, Guan XY, Xie D (2012) Overexpression of EIF5A2 promotes colorectal carcinoma cell aggressiveness by upregulating MTA1 through C-myc to induce epithelial-mesenchymaltransition. Gut 61:562–575